Table 2 Solution type on delta wings of varying ellipticity and Λ = 15 deg at M = 2.68 and α = 6.88 deg

Mesh Wing	12:1	24:1	48:1	Zero thickness
12×36	Attached	Attached	Attached	Separated
24×72	Attached	Separated	Separated	Separated
48×144	Attached	Attached	Separated	Separated
96×288	Attached	Attached	Separated	Separated

the crossflow shock and leeside vortex. Table 2 illustrates solution type for these wings at M = 2.68. For each mesh, decreasing the wing thickness results in transition from an attached to a separated solution. These observations are consistent with cases 1 and 3, or 4 and 6, of Table 1. Here increased tip error is seen to increase the flowfield circulation, which in the case of a thin wing, promotes separation.

Concluding Remarks

This study has examined the conditions under which separated and attached Euler wing solutions occur and has traced the evolution of each flowfield type. In addition, a numerical study on the effect of accuracy on the solution type has been concluded. Based on these results the following conclusions can be drawn: 1) Euler solution type is determined by a transient shock-vortex interaction. A separated solution occurs in response to the formation of a strong crossflow shock. 2) The Mach number and incidence range for which attached and separated Euler solutions occur is qualitatively similar to the vortex and crossflow shock dominated regimes observed in experiment. However, the location of the boundary between these two types of solutions is sensitive to numerical scheme and mesh size. 3) Euler solution type is influenced by a balance among the errors committed at different locations in the flowfield, not by error level alone. Decreased accuracy on the leeside of the wing promotes attached solutions, while decreased accuracy near the tip favors separated solutions. The last conclusion bears upon the differences noted in the performance of central and upwind schemes.[5] These methods add a different balance of errors to the tip and lee regions of the flowfield.

Acknowledgments

This work was supported by the NSWC Independent Research Fund and NAVAIR. The project monitor was Dale Hutchins (AIR-932J).

References

[1]Miller, D. S., and Wood, R. M., "Leeside Flows over Delta Wings at Supersonic Speeds," *Journal of Aircraft*, Vol. 21, No. 9, 1984, pp. 680–686.

[2]Newsome, R. W., and Kandil, O. A., "Vortical Flow Aerodynamics—Physical Aspects and Numerical Simulation," AIAA Paper 87-0205, Jan. 1987.

[3]Newsome, R. W., "Euler and Navier Stokes Solutions for Flow over a Conical Delta Wing," *AIAA Journal*, Vol. 24, No. 4, 1986, pp. 552–561.

[4]Kandil, O. S., and Chang, A., "Influence of Numerical Dissipation in Computing Supersonic Vortex-Dominated Flows," AIAA Paper 86-1073, May 1986.

[5]Newsome, R. W., and Thomas, J. L., "Computation of Leading Edge Vortex Flows," Vortex Aerodynamic Conference, NASA Langley Research Center, Hampton, Virginia, Oct. 1985.

[6]Wardlaw, A. B., Jr., and Davis, S. F., "A Second Order Godunov Method for Supersonic Tactical Missiles," Naval Surface Warfare Center TR 86-506, Dec. 1986.

[7]Wardlaw, A. B., Jr., and Davis, S. F., "Euler Solutions for Delta Wings," AIAA Paper 89-3398, Aug. 1989.

Vertex-Based Finite-Volume Solution of the Two-Dimensional Navier-Stokes Equations

Sunil Kumar Chakrabartty*
National Aeronautical Laboratory, Bangalore, India

Introduction

PAST experiences in solving inviscid flows by the Euler equations provide many opportunities for exploring possible Navier-Stokes solvers. The finite-volume spatial discretization with the Runge-Kutta time-stepping scheme developed for the Euler equations has been successfully extended by Swanson and Turkel[1] to the computation of viscous flows. Their formulation for the finite-volume scheme is of the cell-centered type, where the flow quantities are associated with the center of a cell in the computational mesh and the fluxes across the cell boundaries are calculated using arithmetic means of values in the adjacent cells. The main advantage of the finite-volume method is its flexibility of treating arbitrary geometries. The cell-centered scheme loses its accuracy with grid stretching and skewness.[2] The nodal point discretization, where the flow quantities are ascribed to the corners of the cell, can give better accuracy for the highly stretched and skewed grids[2,3] that are necessary for viscous flow computations. The surface boundary conditions can be satisfied exactly at the vertices along the body surface, and the pressure on the wall can be computed directly by this scheme, whereas an extrapolation is necessary if one uses the cell-centered scheme. A nodal point finite-volume space discretization scheme[3,4] has been used here to solve the two-dimensional Reynolds-averaged Navier-Stokes equations with a thin-layer type of approximation and a simple two-layer algebraic[5] eddy viscosity model. In the present work, the efficiency of the Runge-Kutta scheme and the benefit of convergence acceleration techniques have also been utilized. The results obtained for turbulent flow past a NACA 0012 airfoil have been compared with available numerical and experimental results.

Governing Equations and Boundary Conditions

The Navier-Stokes equations representing the conservation laws have been considered here in integral form[1] for its ability to treat flow discontinuities automatically. To complete the set of equations for a compressible fluid, a thermodynamic equation of state, Stokes' hypothesis, and Sutherland's law have been considered along with the constant Prandtl number assumption.[3,4]

For turbulent flows the compressible Reynolds-averaged Navier-Stokes equations exhibit a term by term correspondence with their laminar flow counterparts, except that the stress tensor is augmented by the Reynolds stress tensor and the heat flux vector is augmented by the additional turbulence heat flux. To close the time-averaged equations in turbulent flow, the two-layer algebraic eddy viscosity model of Baldwin and Lomax[5] has been used.

The boundary conditions are that the velocity components must be zero (no slip) at the body surface, and the wall temperature is either prescribed or its normal derivative is zero (adiabatic wall, present case). A continuity condition has been

Received Jan. 28, 1989; revision received Dec. 5, 1989.

*Scientist, Computational and Theoretical Fluid Dynamics Division.

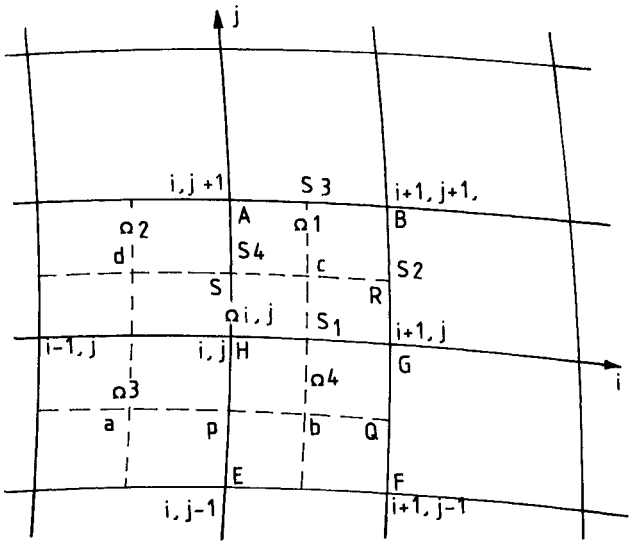

Figs. 1 Finite-volume mesh for nodal point scheme.

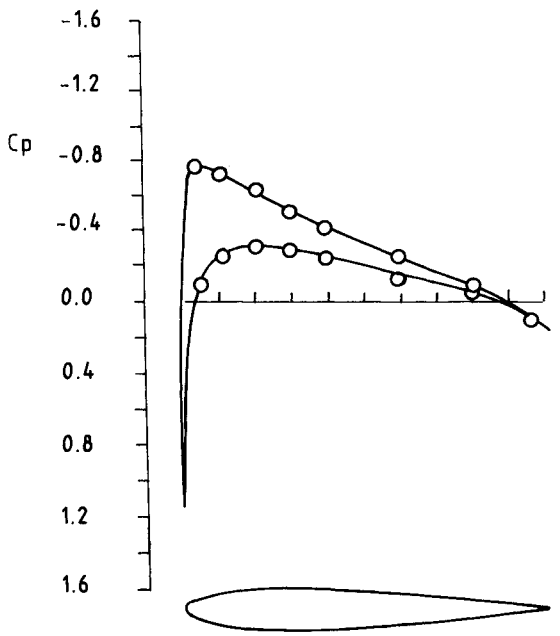

Fig. 2 Comparison of pressure distribution for turbulent flow past a NACA 0012 airfoil; $M_\infty = 0.50$, $\alpha = 1.77$ deg, $Re = 2.91 \times 10^6$.

used along the cut boundary in the computational domain. At the far-field boundary, the viscous effects are assumed to be negligible. The treatment of the far-field boundary in the present analysis is based on Riemann invariants for the one-dimensional flow normal to the boundary. To reduce the extent of the far-field boundary in an asymmetric flow with circulation, the following modification has also been tried here. The effect of a single vortex in compressible medium centered at the airfoil has been added to the freestream flow, and the modified freestream values have been added to compute the Riemann invariants.[4]

Solution Process and Algorithm

To solve the Navier-Stokes equations numerically, a semi-discretization is used that completely separates the discretization of space and time derivatives. To simulate the wake in a better way, the present computations are carried out with algebraically generated C-type body-fitted grids. Once the Cartesian coordinates of the four vertices of every cell are given, the Euler fluxes across the four neighboring cells Ω_1, Ω_2, Ω_3, and Ω_4 can be calculated directly from the flow variables defined at corner points (Fig. 1). To compute the viscous fluxes, Green's theorem has been used to get the first derivatives at the midpoints of the cell boundaries. The scheme can be summarized as follows:

1) Calculate first derivatives of all of the flow variables at $(i+\frac{1}{2}, j)$ using the full control volume $PQRS$ for all (i,j).

2) Calculate the stress tensors and flux terms.

3) Find the difference of flux quantities across two surfaces AB and HG to get the viscous flux over the cell $HGBA$.

4) Add these to the corresponding Euler fluxes for the same cell.

Table 1 Comparison of aerodynamic coefficients for turbulent flow over a NACA 0012 airfoil[a]

Method	Remarks	Mesh	CL	CD	CM
Ref. 1	Finite-volume	120×50	0.198	—	—
C-type	Runge-Kutta				
Ref. 6	Experiment		0.195	0.0070	—
Present C-type	Without effect of vortex at far field; 1500 iterations	131×61	0.1929	0.0131	0.0070
	With effect of vortex at far field, 2000 iterations	131×61	0.2071	0.0128	0.0072
	Without effect of vortex at far field, 1000 iterations	165×61	0.1978	0.0096	0.0064
	Without effect of vortex at far field, 4000 iterations	165×61	0.208	0.0081	0.0058

[a] $M_\infty = 0.50$, $\alpha = 1.77$ deg, $Re = 2.91 \times 10^6$

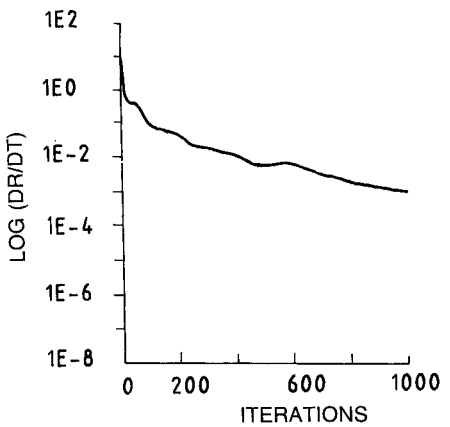

Fig. 3 Convergence history for turbulent flow past a NACA 0012 airfoil; $M_\infty = 0.50$, $\alpha = 1.77$ deg, $Re = 2.91 \times 10^6$ (165×61 grid).

5) Take the average of the four neighboring cells of the point (i,j) to get the net flux across $\Omega_{i,j}$.

It is to be noted that streamwise-like differences are neglected at the second stage in this process (neglecting the diffusion), where in Ref. 1 these were neglected even at the first stage (thin-layer approximation). The resulting system of ordinary differential equations in time is then solved using an explicit five-stage Runge-Kutta time-stepping scheme. Second- and fourth-order artificial dissipation terms[1] have been added for numerical stability. To accelerate the rate of convergence, local time stepping, enthalpy damping, and residual smoothing[1,3] have been applied.

Results and Discussion

Turbulent flow past a NACA 0012 airfoil has been considered at freestream Mach number $M_\infty = 0.5$, angle of attack $\alpha = 1.77$ deg, and freestream Reynolds number $Re = 2.91 \times 10^6$. In the present computation, 165×61 cells were taken with minimum height of the cell near the boundary $Y_{min} = 0.0005$, such that 10–15 cells were accommodated inside the boundary layer. The CPU time taken for the 1000 iterations required for the solution to converge on a CRAY-1 computer is 428 s. The effect of using a vortex at the airfoil for the far-field boundary condition is shown in Table 1 along with a comparison of the aerodynamic coefficients. In all of the computations made so far, no noticeable difference has been observed in the final pressure distribution on the airfoil. Figure 2 shows a representative pressure distribution with good agreement between the computed and experimental results.[6] The incorporation of the vortex results in a higher lift. Oscillatory behavior was observed in convergence histories for 131×61 mesh points in both the cases of with and without considering the effect of a vortex in the far field after about 500 iterations. A smooth convergence has been achieved by using 165×61 mesh points without considering the effect of the vortex. The computations were continued up to 4000 iterations, and the convergence history is shown in Fig. 3. Consideration of the effect of a vortex leads to an unsteady solution in this case.

Acknowledgment

This work contains a part of the work done by the author from November 1986 to August 1987 at the Institute of Design Aerodynamics, DFVLR, Braunschweig, under a joint collaboration program between the Council of Scientific and Industrial Research (India) and Deutsche Forschungs und Versuchsanstalt für Luft und Raumfahrt (West Germany). The valuable discussions the author had with Dr. Anand Kumar and Dr. P. K. Dutta of the National Aeronautical Laboratory, Bangalore, are gratefully acknowledged.

References

[1]Swanson, R. C., and Turkel, E., "A Multistage Time Stepping Scheme for the Navier-Stokes Equations," AIAA Paper 85-0035, Jan. 1985.

[2]Rossow, C., "Comparison of Cell Centre and Cell Vertex Finite Volume Schemes," *Proceedings of 7th GAMM Conference,* 1987.

[3]Chakrabartty, S. K., "Numerical Solution of Two-Dimensional Navier-Stokes Equations by Finite Volume Method," National Aeronautical Lab., Bangalore, India, NAL-PD-FM 8726, also DFVLR-IB-129-87/23, 1987.

[4]Chakrabartty, S. K., "Numerical Solution of Navier-Stokes Equations for Two Dimensional Viscous Compressible Flows," *AIAA Journal,* Vol. 27, No. 7, 1989, pp. 843–844.

[5]Baldwin, B. S., and Lomax, H., "Thin Layer Approximation and Algebraic Model for Separated Turbulent Flows," AIAA Paper 78-257, Jan 1978

[6]Thibert, J. J., Granjacques, M., and Ohman, L. H., "NACA 0012 airfoil," Experimental data base for computer program assessment, AGARD-AR-138, May 1979.

Formation of Secondary Vortex During Vortex-Wedge Interaction

Duck-Joo Lee* and Young-Nam Kim†
Korea Advanced Institute of Science and Technology
Cheong-Ryang, Seoul, Korea

Introduction

VORTICAL flows interacting with bodies have been studied by many researchers as reviewed by Rockwell.[1] These flows cause unsteady loading and/or noise generation in a number of cases; helicopter rotors, marine propellers, supersonic intakes, and cavities, etc. In general, when an incident vortex nears the leading edge of a wedge, the vortex distorts and a secondary vortex is shed near the leading edge due to significant changes in the local angle of attack.

The vortex-wedge iteraction was first studied experimentally by Ziada and Rockwell.[2] In that study, interactions between a row of vortices in the mixing layer and the leading edge of a wedge were investigated. It was found that the transverse (vertical) position of the incident vortex with respect to the leading edge plays an important role during the interactions. This type of interaction was calculated by Conlisk and Rockwell[3] with a point vortex past a rectangular corner. However, this point vortex model could not simulate either the distortion of the vortex or the surface pressure fluctuations on the body when the initial transverse offset is small. The distortion of the incident vortex can be well simulated by modeling the vortex core as multiple vortex elements that are free to move. This vortex core model was considered by the author[4,5] for blade-vortex interaction assuming no flow separation near the leading edge of the airfoil. For the case of vortex-wedge interaction, it is likely that the separation occurs near the leading edge. Consequently, viscous effects should be considered to simulate the leading-edge separation.

In this paper, an attempt has been made to simulate the generation of the secondary vortex near the leading edge of the wedge as well as the distortion of the incident vortex convecting toward the wedge by using Euler-Lagrangian method. A single vortex having a constant vorticity distribution in the core, i.e., a Rankine vortex, is used here as the incident vortex instead of a row of vortices.[2] A hybrid vortex sheet-random vortex method[6] is used to account for viscous effects near the body surface. The velocity field around the wedge is calculated by using a fast vortex method[7,8] rather than a direct discrete vortex method which requires much more computation time. The fast vortex method, originally developed for a rectangular grid, is applied here to a body-fitted coordinate system.

Numerical Method

The incompressible, two-dimensional, Navier-Stokes equations can be wriiten in the form

$$\frac{\partial \xi}{\partial t} + \boldsymbol{u} \cdot \nabla \xi = \frac{1}{Re} \nabla^2 \xi \tag{1}$$

$$\nabla \cdot \boldsymbol{u} = 0 \tag{2}$$

Received Aug. 22, 1989; revision received Dec. 3, 1989.

*Assistant Professor, Department of Aerospace Engineering. Member AIAA.

†Graduate Student; currently at Samsung Aerospace.